Reconfigurable Stepped-Impedance Slotline Power Dividers

Sheng-Loke Lim, Eng-Hock Lim[*]**, and Fook-Loong Lo**

Abstract—For the first time, the higher-ordered modes of a stepped-impedance slotline resonator are closely combined for designing the broadband in-phase and out-of-phase power dividers. It was found that the output phases of the two modes can be easily reversed at the same time by changing the direction of their feeding currents. For this configuration, interestingly, a multifunctional power divider which is reconfigurable to produce either in-phase or out-of-phase signals can be easily designed from its passive counterparts by incorporating multiple RF diodes into the output feedlines, leading to significant cost saving and high compactness. The design procedure and equations of the power-dividing structures are discussed.

1. INTRODUCTION

Microstrip slotline was first proposed by Cohn in the late 60s [1]. It is an alternative to transmission line where narrow wave-guiding slots and gaps are etched on a metal layer laminated on dielectrics. Cohn also showed that the use of high-permittivity substrate was helpful for minimizing radiation in slot [2], making such structure useful for non-radiating microwave circuits. In most cases, a microstrip slot is usually made much smaller than its operation wavelength so that fields are closely confined. The characteristics of the microstrip slotline have also been analyzed in [3].

Since the early 90s, microstrip slotline has been extensively deployed for making microwave components such as antennas [4–6] and couplers [7, 8]. In [9], it was found that an additional resonance could be excited by feeding a high-impedance stubline near to the slot edge, combining with its fundamental slot mode to provide broad bandwidth. The slotline with stepped-impedance shape was proposed in [10] to excite four resonant modes, aiming at achieving ultra-wideband operation. Coupled slotlines were first introduced by [11] for designing magic T, where the authors made use of the two orthogonal modes (odd and even) of this structure to design an 180° hybrid. It was recently found that slotline resonator can also be incorporated with substrate-integrated waveguide [12] for improving its Q factor.

Multifunctional components have been of great recent interest because of their various advantages such as providing compact size and low cost. A myriad of multiple functions have been explored for various couplers. It was shown that a wideband 180° hybrid, which is able to give in-phase (sigma) and out-of-phase (delta) wideband outputs at the same time, can be designed by using the microstrip-slot technology [13–15]. Making a slot resonator multifunctional is very welcome as it has a low Q factor, which is good for achieving wide bandwidth.

In this paper, the higher-ordered modes of the stepped-impedance slotline resonator are first deployed for designing two wideband passive power dividers. In-phase and out-of-phase operations are easily obtainable by feeding the slotline resonator in different directions. Then, the power dividing structure is made multifunctional by incorporating multiple RF PIN diodes into the feedlines of the stepped-impedance slotline resonator. In this case, the slotline power divider can be configured to produce either in-phase or out-of-phase output signals.

2. DESIGN METHODOLOGY

First, a simple stepped-impedance slotline resonator, with the configuration shown in Figure 1(a), is characterized as it will be used for designing the proposed power dividers. It is made on a substrate with dielectric constant of $\varepsilon_r = 3.38$ and thickness of 1.524 mm, with other design parameters given by: $L = 24$ mm, $d = 0.6$ mm, $l_1 = 12$ mm, $l_2 = 15.5$ mm, $a_1 = 9$ mm, and $b_1 = 9.5$ mm. Ansoft HFSS is used for conducting simulations, and experimental results are measured by using the R&S$^\circledR$ ZVB8 Vector Network Analyzer (VNA). Adaptive solution method was used in the simulations [16]. The S-parameters were calculated iteratively until they have reached an error of no more than 2% at 5 GHz. Later, the result was used to extrapolate the data points from 2 GHz to 7 GHz. Automatic meshing procedure was activated and an additional 20% of tetrahedras would be added if the previous solution did not get converged. With reference to the figure, the configuration consists of a hook-shaped microstrip feedline on the top surface of a grounded substrate along with a stepped-impedance slotline resonator which is etched on the ground on the reverse. The effect of the central slot width (W) is now studied. For the case $W = d = 0.6$ mm, as can be seen in Figure 1(b), two resonances are observed at $f_1 = 4.16$ GHz and $f_2 = 6.4$ GHz. It is worth-mentioning that the spectrum is clean below f_1 with no other resonances. With W increasing from 0.6 to 16 mm, the second resonance reduces down to 5.35 GHz. The same phenomenon is also observed for the first mode, but with lesser decrement. Figure 2 shows the electric field distribution on the slotline for $W = 16$ mm. It is observed that the first resonating mode ($f_1 = 3.91$ GHz) has one null point at the center rolling with two complete cycles of standing waves, showing that this is a higher-order mode. The resonant frequency (f_1) can be related to the slot length by $(l_1 + l_2 + L) = c/f_1$, where c is speed of light. Two nulls (or three complete standing

(a)   (b)
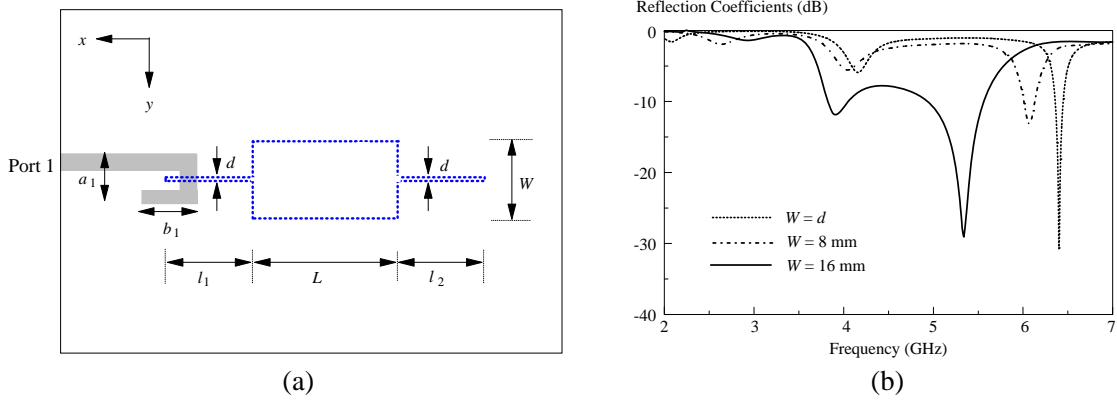
Figure 1. (a) The configuration of a simple stepped-impedance slotline resonator. (b) Reflection coefficient for different slot widths (W).

(a)   (b)
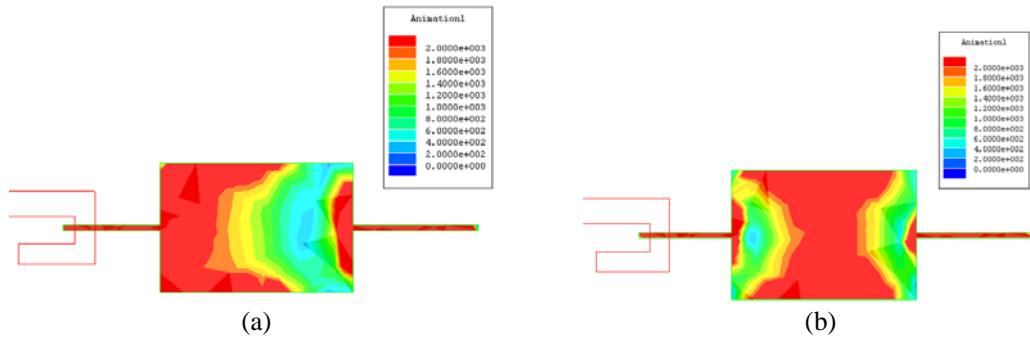
Figure 2. The electric field distributions for $W = 16$ mm at the two modes, (a) $f_1 = 3.91$ GHz and (b) $f_2 = 5.35$ GHz.

waves) are observed along the slotline for the second resonance mode ($f_2 = 5.35\,\text{GHz}$), showing that it is also a higher-order mode which can be calculated using $(l_1 + l_2 + L) = 1.5c/f_2$. From the above-given equations, the calculated resonant frequencies are $f_1 = 3.93\,\text{GHz}$ and $f_2 = 5.9\,\text{GHz}$, pretty close to the simulated ones ($f_1 = 4.16\,\text{GHz}$ and $f_2 = 6.4\,\text{GHz}$).

3. CIRCUIT CONFIGURATION

The stepped-impedance slotline resonator (Figure 1) is now used to design two different power-dividing structures, both of which are fed by $50\,\Omega$ microstrips. The proposed configurations are 3-port passive power dividers, shown in Figures 3(a) and (b), optimized to provide in- and out-of-phase power divisions, respectively. It is found that the phase polarity of the output signal is changeable by inverting the feeding direction of the hook-shaped microstrip. The detailed design parameters for the in-phase power divider are given by $W_1 = 16\,\text{mm}$, $L_1 = 24\,\text{mm}$, $a_1 = 9\,\text{mm}$, $a_2 = a_3 = 10\,\text{mm}$, $b_1 = 0.6\,\text{mm}$, $b_2 = b_3 = 0.7\,\text{mm}$, $b_4 = 0.9\,\text{mm}$, $c_1 = 7.7\,\text{mm}$, $c_2 = 18.05\,\text{mm}$, $c_3 = 15.35\,\text{mm}$, $c_4 = 8.45\,\text{mm}$, $d_1 = 12\,\text{mm}$, $d_2 = d_3 = 14.2\,\text{mm}$, $d_4 = 15.5\,\text{mm}$, $l_1 = l_3 = 9.5\,\text{mm}$, and $l_2 = 9\,\text{mm}$. Also given are the optimized parameters of the out-of-phase power divider: $W_1 = 16\,\text{mm}$, $L_1 = 24\,\text{mm}$, $a_1 = 9\,\text{mm}$,
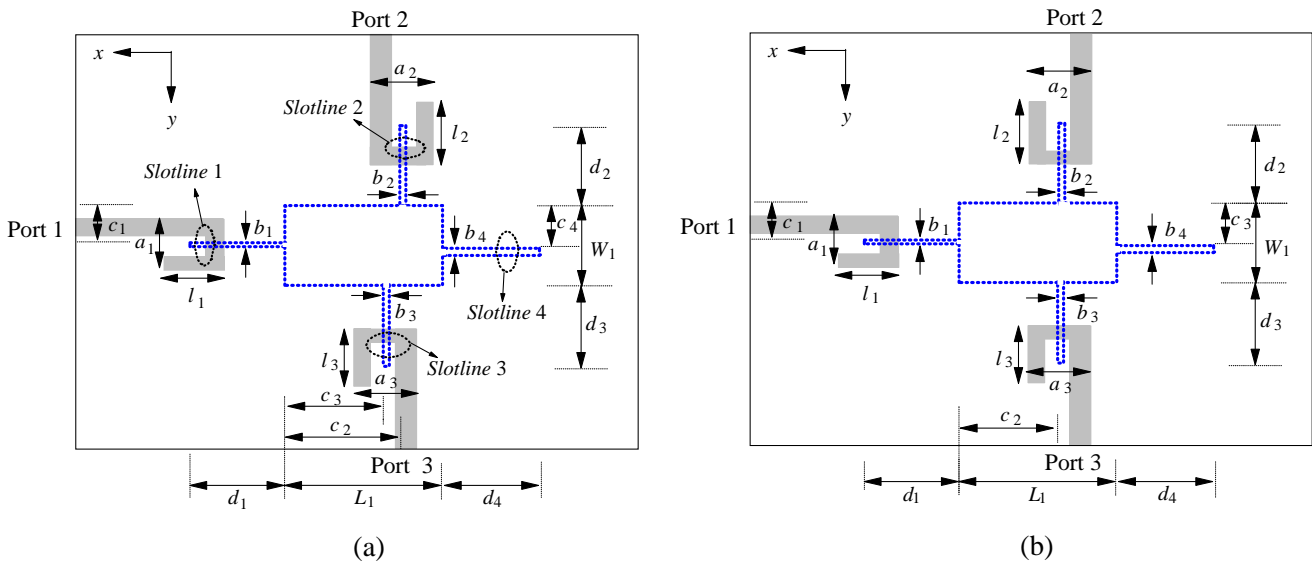
Figure 3. Configurations of the proposed passive power dividers. (a) In-phase power divider. (b) Out-of-phase power divider.

Figure 4. Photographs of the passive in-phase power divider. (a) Top view. (b) Bottom view.

Figure 5. Photographs of the passive out-of-phase power divider. (a) Top view. (b) Bottom view.
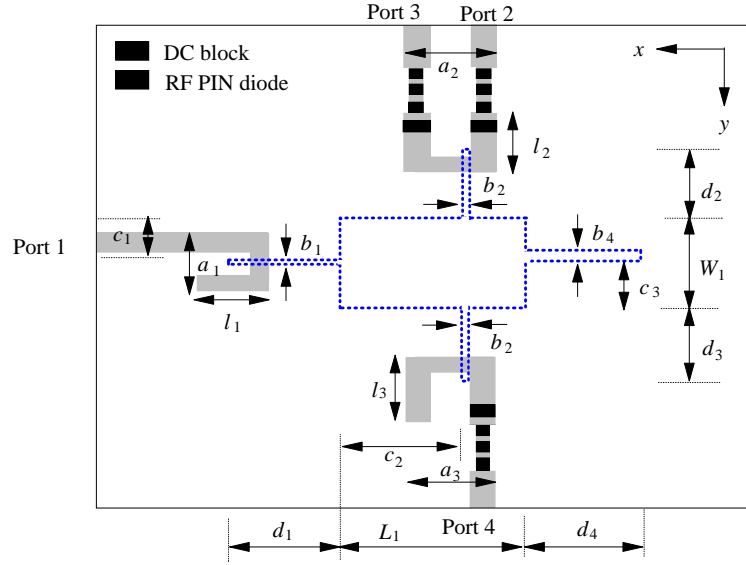
Figure 6. The configuration of proposed 4-port reconfigurable power divider.

$a_2 = a_3 = 10$ mm, $b_1 = 0.2$ mm, $b_2 = b_3 = 0.7$ mm, $b_4 = 1$ mm, $c_1 = 7.2$ mm, $c_2 = 16$ mm, $c_3 = 8.3$ mm, $d_1 = 12.3$ mm, $d_2 = 13.2$ mm, $d_3 = 13$ mm, $d_4 = 18$ mm, $l_1 = l_3 = 9.5$ mm, and $l_2 = 10$ mm. Figures 4 and 5 show the top- and bottom-view photographs of the fabricated in-phase and out-of-phase power dividers, respectively.

The in-phase and out-of-phase passive power dividers are then incorporated with RF diodes to design a reconfigurable power divider. It will be shown that the proposed circuit configuration (in Figure 6) can generate either in-phase or out-of-phase outputs in a single module. Referring to Figure 6, each output port (Port 2, 3, or 4) has two RF diodes in order to achieve an isolation level of greater than -20 dB at the OFF state. For the in-phase case, the input microwave signal is first given to Port 1 and it is channeled to outputs at Ports 3 and 4. The unused port (Port 2) is disconnected. On the other hand, Port 1 feeds the output signals to Ports 2 and 4 for obtaining out-of-phase output signals, with Port 3 disconnected. This is very versatile as now the same configuration can be made a multifunctional component, leading to significant cost saving. The detailed design parameters for the reconfigurable power divider are given by $W_1 = 16$ mm, $L_1 = 24$ mm, $a_1 = 9$ mm, $a_2 = a_3 = 11.5$ mm, $b_1 = 0.2$ mm, $b_2 = b_3 = 0.7$ mm, $b_4 = 1$ mm, $c_1 = 7.9$ mm, $c_2 = 16.5$ mm, $c_3 = 9$ mm, $d_1 = 12.3$ mm, $d_2 = 12$ mm, $d_3 = 12$ mm, $d_4 = 16$ mm, $l_1 = 9.5$ mm, $l_2 = 10$ mm, and $l_3 = 9$ mm. Figure 7 shows the photographs of the top- and bottom surfaces of the fabricated prototypes.

(a)   (b)
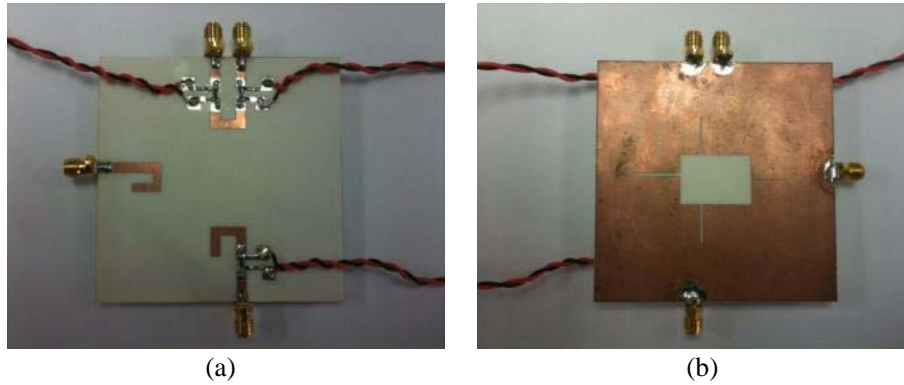
Figure 7. Photographs of the reconfigurable power divider. (a) Top view. (b) Bottom view.

(a)   (b)
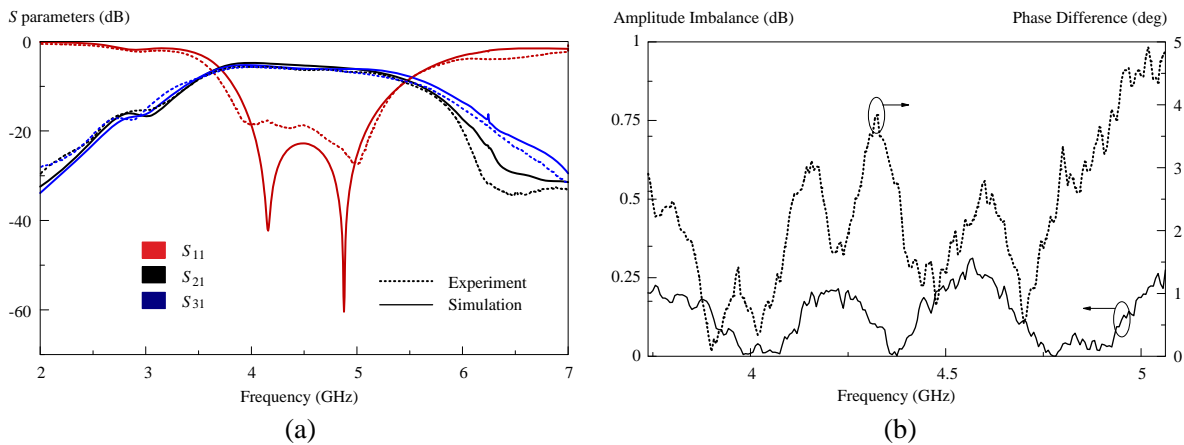
Figure 8. (a) Simulated and measured S parameters, (b) calculated (from measured results) amplitude imbalance and phase difference of the in-phase passive power divider.

4. RESULTS AND DISCUSSION

When simulating the in-phase power divider, the S-parameters were found to be able to reach an accuracy of 1.9951% with a total of 25788 tetrahedras after 11 iterations. Figures 8(a) and (b) show the measured and simulated S parameters as well as the calculated (from measured results) amplitude imbalance and phase difference of the in-phase passive power divider. It has a measured passband of 3.74 GHz–5.4 GHz and a fractional bandwidth (FBW) of 36.39% (simulation: 3.84 GHz–5.41 GHz and FBW — 34.04%), with $|S_{11}| \leq -20$ dB, $||S_{21}| - |S_{31}|| \leq 0.3$ dB, and $|\angle S_{21} - \angle S_{31}| \leq 5°$. The maximum insertion losses of S_{21} and S_{31} are measured to be -5.62 and -5.68 dB, respectively. Higher insertion loss is observed due to residual radiation of the microstrip-to-slot-transition [14]. The experimental result has slightly larger FBW than the simulated one.

The measured and simulated S parameters as well as the calculated (from measured results) amplitude imbalance and phase difference of the out-of-phase power divider are shown in Figures 9(a) and (b). The simulation process has converged to achieve an accuracy of 1.6826% after 10 iterations, with a total of 19148 tetrahedras. It has a measured passband of 3.66 GHz–4.81 GHz and a FBW of 27.01% (simulation: 3.84 GHz–5.0 GHz and FBW — 26.26%), with $|S_{11}| \leq -10$ dB, $||S_{21}| - |S_{31}|| \leq 0.7$ dB and $|\angle S_{21} - \angle S_{31}| \leq 180 \pm 3°$. The maximum insertion losses of S_{21} and S_{31} are measured to be -5.75 and -5.9 dB, respectively, at the resonances. Measurement result also shows that the proposed power divider has two resonance modes at 3.98 GHz and 4.41 GHz (simulation: — 4.14 GHz and 4.57 GHz). Good agreement is found between the simulated and measured results.

The reconfigurable power divider is first configured into in-phase mode. Figures 10(a) and (b)
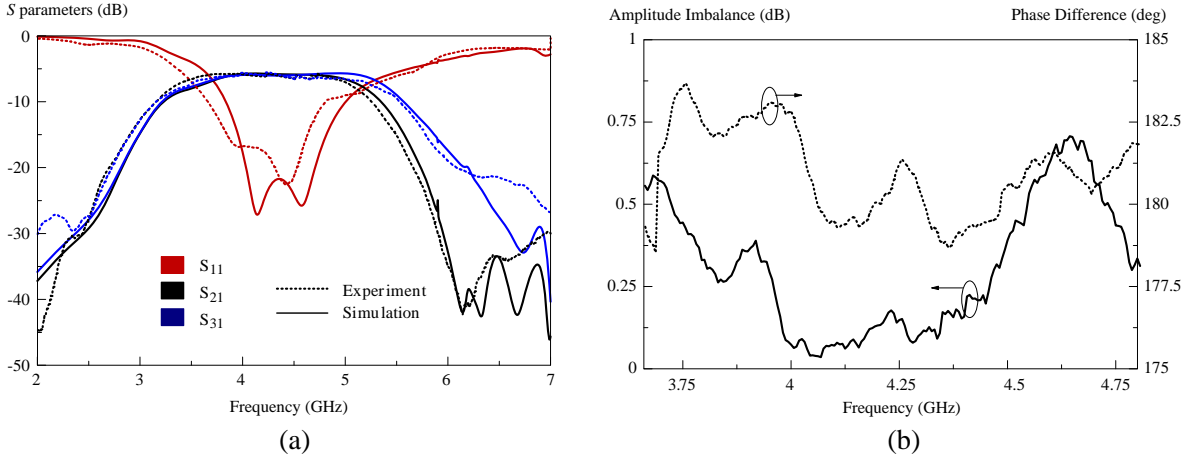
Figure 9. (a) Simulated and measured S parameters, (b) calculated (from measured results) amplitude imbalance and phase difference of the out-of-phase passive power divider.
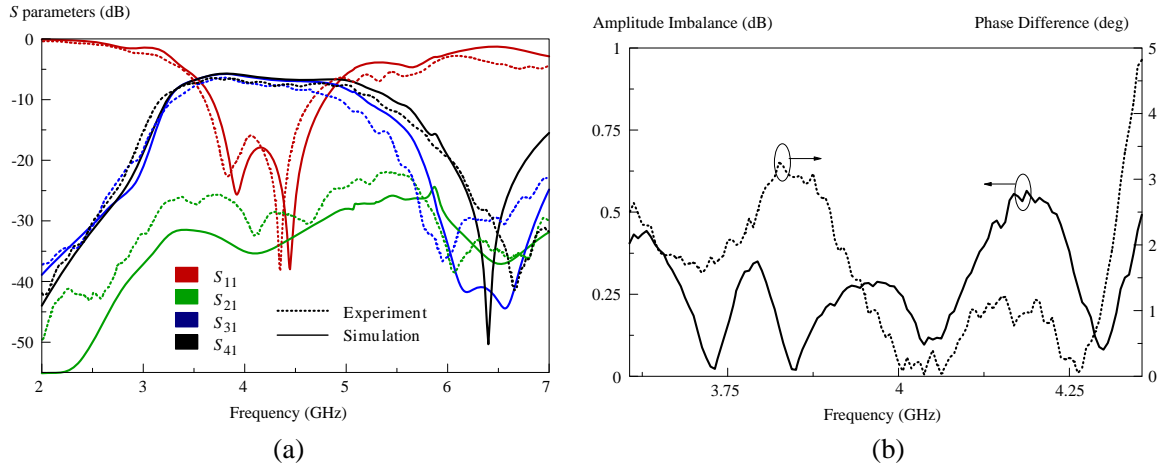
Figure 10. (a) Simulated and measured amplitude response, (b) calculated (from measured results) amplitude imbalance and phase difference of the reconfigurable in-phase power divider (Figure 6).

depict the simulated and measured S parameters as well as the calculated (from measured results) amplitude imbalance and phase difference. The measured passband is 3.61–4.36 GHz (simulation: 3.67–4.78 GHz) with a FBW of 19% (simulation: 26%). It can be seen from the figure that the measured and simulated center frequencies are 3.98 GHz and 4.23 GHz, respectively, showing reasonable agreement with an error of 6.28%. This result is acceptable for the active case as the tolerance of active devices is usually controllable within 10%. With the use of two diodes, as can be seen in Figure 10(b), the isolation level ($|S_{21}|$) is managed well below -25 dB across the entire passband. The amplitude imbalance and phase difference between the two output ports (Port 3 and Port 4) fall within ≤ 0.6 dB and $\pm 4.8°$, respectively, both of which are calculated from measurements.

Next, the reconfigurable power divider is made to operate in the out-of-phase mode by turning OFF the diodes at Port 3. Figure 11(a) shows the measured and simulated amplitude responses of the out-of-phase configuration. The measured and simulated center frequencies are 3.98 and 4.14 GHz, respectively, with an error of 4.02%. The measured FBW (18.67%) is lower than the simulated one (23.8%). With reference to the figure, the isolation level ($|S_{31}|$) is measured at ~ -20 dB in the passband. The calculated (from measured results) amplitude imbalance and phase difference of the out-of-phase configuration are shown in Figure 11(b), and are less than 0.54 dB and within $180 \pm 4.9°$ across the entire passband.
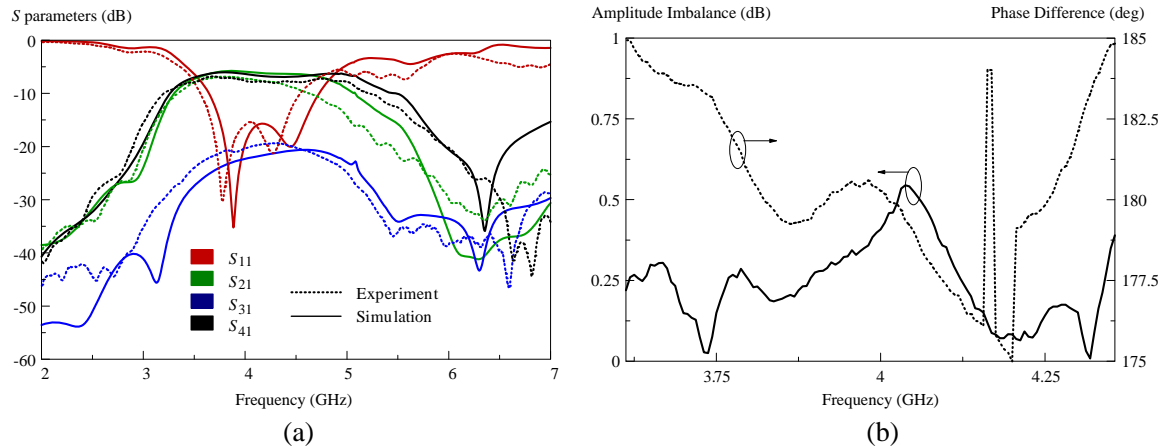
Figure 11. (a) Simulated and measured amplitude response, (b) calculated (from measured results) amplitude imbalance and phase difference of the reconfigurable out-of-phase power divider (Figure 6).

5. CONCLUSION

An in-phase passive power divider, an out-of-phase passive power divider, and a reconfigurable active power divider have been designed using the proposed stepped-impedance slotline resonator. In the first part, the passive components are designed and optimized. It was found that the phase polarity of the output signal is changeable by inverting the feeding direction of the hook-shaped microstrip feedline. Next, the in-phase and out-of-phase passive power dividers are combined to form a reconfigurable power divider. By incorporating several RF PIN diodes into the output feedlines, the proposed active power divider is able to generate the in-phase or out-of-phase outputs. All the measured results show reasonable agreement with the simulated ones.

ACKNOWLEDGMENT

REFERENCES

1. Cohn, S. B., "Slot line — An alternative transmission medium for integrated circuits," *International Microw. Symp.*, 104–109, 1969.

2. Cohn, S. B., "Slot line on a dielectric substrate," *IEEE Trans. Microw. Theory Tech.*, Vol. 17, No. 10, 768–778, 1969.

3. Mariani, E. A., C. P. Heinzman, J. P. Agrios, et al., "Slot line characteristics," *IEEE Trans. Microw. Theory Tech.*, Vol. 17, No. 12, 1091–1096, 1969.

4. Elazar, G. and M. Kisliuk, "Microstrip linear slot array antenna for X-band," *IEEE Trans. Antennas Propag.*, Vol. 36, No. 8, 1144–1147, 1998.

5. Iwasaki, H., K. Kawabata, and K. Yasukawa, "A circularly polarized microstrip antenna using a crossed-slot feed," *International Antennas Propag. Symp.*, 807–810, 1990.

6. Itoh, K. and M. Yamamoto, "A slot-coupled microstrip array antenna with a triplate line feed where parallel-plate mode is suppressed efficiently," *International Antennas Propag. Symp.*, 2135–2138, 1997.

7. Tanaka, T., K. Tsunoda, and M. Aikawa, "New slot-coupled directional couplers between double-sided substrate microstrip lines, and their applications," *International Microw. Symp.*, 579–582, 1998.

8. Ho, C. H., L. Fan, and K. Chang, "Slot-coupled double-sided microstrip interconnects and couplers," *International Microw. Symp.*, 1321–1324, 1993.

9. Behdad, N. and K. Sarabandi, "A wide-band slot antenna design employing a fictitious short circuit concept," *IEEE Trans. Antennas Propag.*, Vol. 53, No. 1, 475–482, 2005.

10. Huang, X. D., C. H. Cheng, and L. Zhu, "An ultrawideband (UWB) slotline antenna under multiple-mode resonance," *IEEE Trans. Antennas Propag.*, Vol. 60, No. 1, 385–389, 2012.

11. Aikawa, M. and H. Ogawa, "A new MIC magic-T using coupled slotlines," *IEEE Trans. Microw. Theory Tech.*, Vol. 28, No. 6, 523–528, 1980.

12. Cheng, Y. J., W. Hong, K. Wu, et al., "A hybrid guided-wave structure of half mode substrate integrated waveguide and conductor-backed slotline and its application in directional couplers," *IEEE Microw. Wireless Compon. Lett.*, Vol. 21, No. 2, 66–67, 2011.

13. Bialkowski, M. E. and A. M. Abbosh, "Design of a compact UWB out-of-phase power divider," *IEEE Microw. Wireless Compon. Lett.*, Vol. 17, No. 4, 289–291, 2007.

14. Bialkowski, M. E. and Y. Wang, "Wideband microstrip 180° hybrid utilizing ground slots," *IEEE Microw. Wireless Compon. Lett.*, Vol. 20, No. 9, 495–497, 2010.

15. Bialkowski, M. E. and Y. Wang, "UWB planar out-of-phase Wilkinson power divider utilizing UWB ±90° phase shifters in microstrip-slot technology," *Asia-Pacific Microw. Conference Proceedings*, 1138–1141, 2011.

16. High Frequency Structure Simulator (HFSS), Ansoft, 2015.